Biosensors and Bioelectronics 54 (2014) 273–278

Contents lists available at ScienceDirect

Biosensors and Bioelectronics

journal homepage: www.elsevier.com/locate/bios

Enhanced non-enzymatic glucose sensing based on copper nanoparticles decorated nitrogen-doped graphene

Ding Jiang, Qian Liu, Kun Wang*, Jing Qian, Xiaoya Dong, Zhenting Yang, Xiaojiao Du, Baijing Qiu

Key Laboratory of Modern Agriculture Equipment and Technology, School of Chemistry and Chemical Engineering, Jiangsu University, Zhenjiang 212013, PR China

ARTICLE INFO

Article history:
Received 13 August 2013
Received in revised form
18 October 2013
Accepted 2 November 2013
Available online 12 November 2013

Keywords:
Nitrogen-doped graphene
Cu nanoparticle
Biosensor
Glucose

ABSTRACT

Copper nanoparticles (NPs) decorated nitrogen-doped graphene (Cu–N-G) was prepared by a facile thermal treatment, and further employed as a novel sensing material for fabricating the sensitive non-enzymatic glucose sensor. Compared with pure Cu NPs, the Cu–N-G showed enhanced electrocatalytic activity to glucose oxidation due to the integration of N-G, which exhibited the oxidation peak current of glucose ca. 23-fold higher than that of pure Cu NPs. The presented sensor showed excellent performances for glucose detection including wide linear range of 0.004–4.5 mM, low detection limit (1.3 μM, $S/N=3$), high sensitivity (48.13 μA mM^{-1}), fast response time (<5 s), good selectivity to the general coexisted interferences, etc. Such properties would promote the potential application of the nitrogen-doped graphene as enhanced materials in fabricating sensors for chemical and biochemical analysis.

1. Introduction

Efficient and highly sensitive detection of glucose concentration is of considerable importance in various fields ranging from medical applications in blood glucose sensing to ecological applications, and various approaches to glucose sensing have been developed including electrochemical, optical, thermometric, and fluorescent sensors (Steiner et al., 2011; Wu et al., 2011; Wang et al., 2013). Among these different types of sensors, amperometric glucose enzymatic sensors are promising due to their simple instrumentation and convenient operation, based on which good selectivity and high sensitivity have been achieved for glucose detection (Delvaux and Champagne, 2003; Qiu et al., 2009; Valentini et al., 2013). However, owing to the intrinsic nature of enzymes, enzymatic glucose sensors can easily be affected by temperature, pH value, humidity, and toxic chemicals (Sun et al., 2011). As an alternative strategy, several functionalized nanomaterials, such as gold nanowire (Cherevko and Chung, 2012), cobalt oxide nanorods (Kung et al., 2011), palladium nanoparticles/carbon nanotubes (Chen et al., 2009) and platinum nanoflowers/graphene oxide (Wu et al., 2013), have been designed and employed as sensing materials for fabricating non-enzymatic glucose sensors during recent years, which overcome the disadvantages of enzymatic glucose sensors to some extent.

Copper and copper oxides based nanomaterials have attracted great attention for non-enzymatic glucose sensor owing to their high electrocatalytic activity, and some other advantages of inexpensive, non-toxic, easily produced and readily stored (Yang et al., 2012). For example, Wang et al. (2010) have fabricated a sensitive non-enzymatic glucose sensor by employing CuO flowers and nanorods as the sensing material; Zhang et al. (2012) reported a sensitive and selective non-enzymatic glucose sensing platform based on the one-dimensional Cu nanowires. Furthermore, in order to improve their catalytic activity, great efforts have been made to combining copper or copper oxides with carbon-based nanomaterials (Kang et al., 2007; Luo et al., 2012; Zhou et al., 2012). For instance, Kang et al. (2007) fabricated a non-enzymatic glucose sensor based on Cu nanoclusters/multiwall carbon nanotube (MWCNT), which exhibited amplified and fast response for electrocatalytic oxidation of glucose by the introduction of MWCNT; Luo et al. (2012) developed a non-enzymatic glucose sensor based on Cu–graphene nanocomposites, and the sensor showed much higher current and more negative onset potential for glucose oxidation than Cu nanoparticles (NPs). All these studies indicated that combining copper or copper oxides with carbon-based nanomaterials could efficiently improve the performance of non-enzymatic glucose sensors, due to the increased electrocatalytic active area and the promoted electron transfer for glucose oxidation of carbon-based nanomaterials (Luo et al., 2012; Zhao et al., 2013).

Most recently, nitrogen-doped graphene (N-G), as a kind of novel carbonaceous derived materials, has received considerable interests by virtue of its excellent properties, such as large

* Corresponding author. Tel.: +86 511 88791800; fax: +86 511 88791708.
E-mail address: wangkun@ujs.edu.cn (K. Wang).

0956-5663/$ - see front matter © 2013 Elsevier B.V. All rights reserved.
http://dx.doi.org/10.1016/j.bios.2013.11.005

functional surface area, high ratio of surface active groups to volume, biocompatible C–N microenvironment, high electrical conductivity and much chemically active sites (Yang et al., 2013a). Furthermore, the latest studies indicated that N-G can provide excellent platforms for loading nanomaterials and improve their catalytic activity. According to Xiong's report (Xiong et al., 2013), Pt/N-G exhibited significantly enhanced catalytic activity for methanol electro-oxidation reaction compared to pure Pt. Borowiec et al. (2013) developed a sensor for electrochemical determination of chloramphenicol based on Au/N-G, which exhibited better electrocatalytic performance for chloramphenicol than Au/graphene. All these results indicated that N-G shows great potential as enhanced materials for fabricating the electrochemical sensing interface, and up to now, it is just the beginning of this fantastic topic.

In this paper, copper NPs decorated nitrogen-doped graphene (Cu–N-G) were prepared by a facile thermal treatment, using N-G as a novel substrate material. Due to the integration of N-G, the as-prepared Cu–N-G showed enhanced electrocatalytic activity to glucose oxidation, which exhibited the oxidation peak current ca. 23-fold higher than that of pure Cu NPs. Furthermore, combining the advantageous features of N-G and Cu NPs, a novel non-enzymatic glucose sensor has been constructed, which showed good performances for glucose sensing with high sensitivity, excellent selectivity, fast response, wide detection range and good stability. In addition, the prepared biosensor can be used for the detection of glucose in real samples with good accuracy, which may find practical applications in the future for the assay of blood glucose.

2. Experimental

2.1. Reagents and chemicals

Graphite was purchased from Qingdao Tianhe Graphite Co., Ltd. D-(+)-Glucose, L-Asorbic (AA), dopamine hydrochloride (DA), 4-acetamidophenol (AP), uric acid (UA) and Nafion (5 wt%) were purchased from Sigma-Aldrich. $Cu(NO_3)_2$, glycine (Gly), NaOH and NaCl were purchased from Sinopharm Chemical Reagent Co., Ltd. Graphene oxide (GO) was prepared using modified Hummers method from graphite powders (Gilje et al., 2007). Unless otherwise stated, reagents were of analytical grade and used as received. All solutions were prepared with double distilled water.

2.2. Apparatus

Characteristics were performed via transmission electron microscopy (TEM, Hitach H800, Japan), scanning electron microscopy (SEM, JEOL JSM-6700, Japan) equipped with an energy-dispersive spectroscopy (EDS, Oxford Inca Energy 400, UK). X-ray diffraction spectra (XRD, Bruker D8 ADVANCE diffractometer, Germany) with Cu Kα ($\lambda = 1.54$ Å) radiation, Raman spectra (RM 2000 microscopic confocal Raman spectrometer, England), X-ray photoelectron spectroscopy (XPS, PHI 5000 VersaProbe, Japan). Electrochemical impedance spectroscopy (EIS) was performed in 0.1 M KCl solution containing 5 mM $Fe(CN)_6^{3-/4-}$ with a frequency range from 0.01 Hz to 10 kHz, and the amplitude of the applied sine wave potential in each case was 5 mV which was taken with a ZENNIUM electrochemical workstation (Zahner Instruments, Germany). The electrochemical experiments were performed with a CHI660 B electrochemical analyzer (Chen Hua Instruments, Shanghai, China). in a conventional three-electrode system where glassy carbon electrode (GCE, 3 mm diameter) was used as working electrode, saturated calomel electrode (SCE) as reference electrode and platinum wire as counter electrode, respectively. Amperometric curves were obtained after adding a glucose solution of certain concentration into 0.1 M NaOH electrolyte under stirring conditions, and then the current in each experiment was recorded when it reached the steady state.

2.3. Preparation of samples

GO was mixed with copper nitrate and Gly at a mass ratio of 1:1:8 (GO:copper nitrate:Gly) in water. The resulting mixture was sonicated for two hours and poured into an alumina crucible. The temperature of the mixture was gradually increased from room temperature to 500 °C under argon atmosphere and maintained for 2 h. Then, the final product was collected from the crucible directly. Similarly, N-G was prepared without adding copper nitrate. The Cu NPs were prepared according to the method described in our previous work (Xu et al., 2011).

2.4. Preparation of the modified electrodes

Prior to modification, the GCE was first polished with sand paper followed by 1.0, 0.3, and 0.05 μm alumina slurry, respectively. After successive sonication in ethanol and double distilled water, the electrode was rinsed with double distilled water and allowed to dry at room temperature. 2 mg mL^{-1} Cu–N-G suspension was prepared by dispersing 1.0 mg Cu–N-G in 0.5 mL ethanol with ultrasonic agitation for about 2 min. Then, the as-prepared Cu–N-G suspension and 30 μL of 5% Nafion were mixed with ultrasonic agitation for 2 min. After that, 6 μL of the suspension was spread evenly onto the pretreated GCE surface and allowed to dry in ambient air for 24 h. Nafion/Cu–N-G modified GCE was thus successfully obtained (denoted as Nafion–Cu–N-G/GCE). For comparison, Nafion–N-G/GCE and Nafion–Cu/GCE were prepared using a similar procedure.

3. Results and discussion

3.1. Characterization of Cu–N-G

The TEM image of Cu–N-G is shown in Fig. 1, and it is obvious that the two-dimensional N-G sheets were well decorated by a large quantity of Cu NPs and both the outline of N-G and Cu NPs could be clearly observed. In addition, the synthesized N-G sheets (Fig. S1) showed a characteristically crumpled and overlapped multilayer surface structure. As shown in Fig. S2A, the Cu NPs with the size of 80–120 nm were uniformly decorated on the surface of N-G, and no free NPs were presented outside the N-G sheets. The morphologies of Cu–N-G were also characterized by SEM. Cu NPs were uniformly distributed on the N-G sheets as shown in Fig. 1B, and in some place, Cu NPs were deposited on both sides of the N-G sheets. EDS spectrum in Fig. S2B further confirmed that Cu NPs were formed on N-G sheets. Besides Cu, the elements of C, N, and O were detected as well. The peaks of C and N belonged to N-G and the existence of oxygen signal was due to the incomplete reduction from GO to N-G.

Further structural characterization of Cu–N-G was performed by XRD. As shown in Fig. 2A, the diffraction peak located at the 2θ value of ~26° was ascribed to the hexagonal structure ((002) plane) of N-G (Xiong et al., 2013). The three major peaks at 43.5°, 50.5° and 74.5° in the range of 40–80° correspond to the (111), (200) and (220) planes of Cu with cubic phase (JCPDS card no. 04-0836), respectively (Xu et al., 2011; Luo et al., 2012; Zhao et al., 2013). These results were consistent with the EDS results, which further confirmed that the Cu NPs were coated on the N-G sheets.

To characterize graphite and graphene materials, Raman scattering has been proved to be an essential tool, particularly for distinguishing ordered and disordered crystal structure of carbon

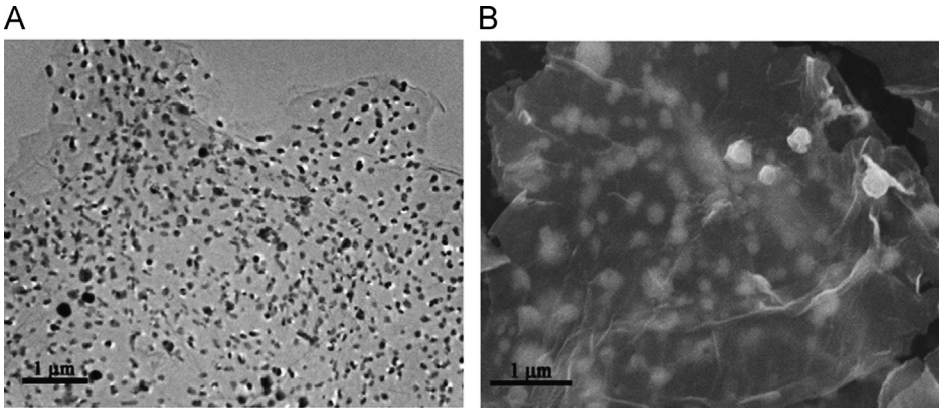

Fig. 1. (A) TEM image of Cu–N-G and (B) SEM image of Cu–N-G.

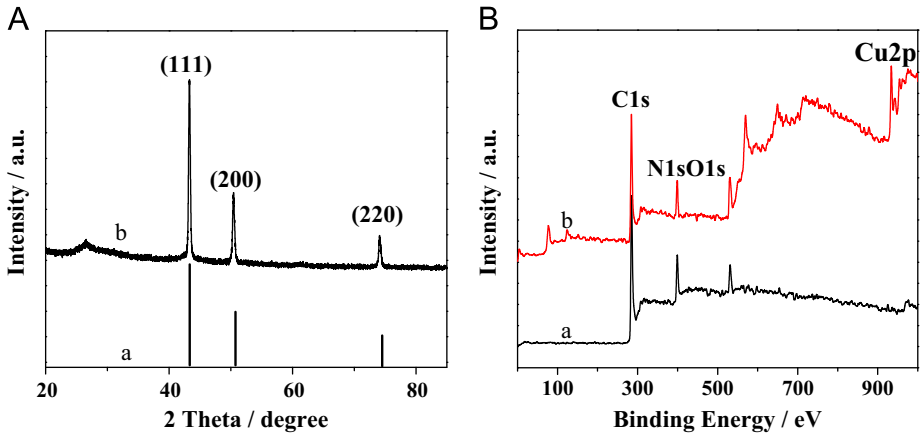

Fig. 2. (A) XRD pattern of JCPDS card no. 04-0836 (a) and Cu–N-G (b). (B) EDS spectrum of Cu–N-G.

and carbon-heteroatom from carbon–carbon bonds. Raman spectra of the as-prepared graphene (a), N-G (b) and Cu–N-G (c) were given in Fig. S3A. For comparison, the spectrum of graphene obtained from thermal reduction of GO under the same conditions was shown in curve a. It is evident that two remarkable peaks of graphene were observed at 1346 cm^{-1} and 1579 cm^{-1}, corresponding to the characteristic D and G bands of carbon materials, respectively. In general, the D band is associated with structural defects, while the G band is the result of the first-order scattering of the E_{2g} mode of sp^2 carbon domains (Guo et al., 2013; Higgins et al., 2013). For N-G (curve b) and Cu–N-G (curve c), the G band shifted to 1584 cm^{-1} and 1587 cm^{-1}, respectively, indicating the insertion of N atoms in graphene (Yang et al., 2013b). Compared with graphene, the N-G and Cu–N-G exhibited strong D band peak at 1346 cm^{-1} due to a high defect density (incorporated N) (Vinayan et al., 2012). Commonly the D/G intensity ratio (I_D/I_G) reflects the defect density in carbon materials. The as-prepared Cu–N-G and N-G were found to have the high I_D/I_G of 1.06 and 1.04, respectively, obviously larger than the I_D/I_G of 0.74 observed for graphene, which was attributed to the structural defects caused by heterogeneous nitrogen atoms insertion into the graphene layers (Jin et al., 2013).

XPS analysis was carried out to further analyze the chemical composition and status of Cu–N-G and N-G. As shown in Fig. 2B, the XPS scan spectra of N-G (a) and Cu–N-G (b) exhibited distinct C1s, N1s and O1s peaks. In the case of Cu–N-G, additional distinct Cu 2p peaks were observed. Moreover, the high-resolution spectrum of Cu 2p (Fig. S3B) obviously showed binding energy peaks at 932.4 and 952.3 eV corresponding to Cu $2p_{3/2}$ and $Cu2p_{1/2}$ photoelectron transitions, respectively, which is characteristic of Cu in the zero-oxidation state (Sreedhar et al., 2008). As shown in Fig. S4, the high resolution N1s spectra for Cu–N-G (a) and N-G (b) show three bands at 398.3, 399.8 and 400.9 eV, corresponding to the pyridinic nitrogen, amino nitrogen and pyrrolic nitrogen, respectively (Vinayan et al., 2012; Xiong et al., 2013;Yang et al., 2013b). Notably, the amount of nitrogen incorporated in N-G was found to be approximately 15% with a high doping level. According to previous studies, the pyridinic nitrogen at graphene can provide a pair of electrons for conjugation with the π-conjugated rings which can introduce electron donor properties to graphene sheets and improve the electrochemical performances of N-G; the pyrrolic nitrogen has higher charge mobility in graphene due to better electron-donor characteristics and enhanced carbon catalytic activity in electron-transfer reactions (Yang et al., 2013b). Therefore, the electrocatalytic activity of Cu–N-G is expected to be better than pure Cu NPs. The C1s XPS spectra of Cu–N-G (c) and N-G (d) in Fig. S4 revealed the formation of various surface groups on the obtained materials which could be reasonably deconvoluted into five components corresponding to the following carbon functional groups: C–C (284.5 eV), C–N (285.9 eV), C–O (286.5 eV), CåO (287.9 eV) and O–CåO (289.1 eV). Furthermore, the O 1 s XPS spectra of Cu–N-G (e) and N-G (f) shown in Fig. S4 could be fit to three constituents: O–C (531.5 eV), OåC (532.6 eV) and O–CåO (533.8 eV) (Yang et al., 2013b; Xiong et al., 2013).

3.2. Electrochemical characterization

EIS is widely used to study features of electrodes to obtain information on electron transfers between the electrolyte and the electrode surface. The EIS normally includes a semicircular part and a linear part. It is usually considered that the semicircle diameter at higher frequencies corresponds to the electron-transfer resistance (R_{et}),

and the linear part at lower frequencies corresponds to the diffusion process (Hu et al., 2012). As shown in Fig. S5, the bare GCE exhibited an almost straight line (curve a), which implied the characteristic of a diffuse limiting step of the electrochemical processes. After dripping Nafion on the surface of the electrode, an obvious interfacial R_{et} was observed (curve b), perhaps due to the Nafion film acting as a barrier and blocking interfacial charge transfer. However, when Nafion–Cu was assembled onto the electrode, the R_{et} was decreased (curve c), which showed that Nafion–Cu was successfully immobilized on the GCE surface (Kang et al., 2007). After the Nafion–Cu–N-G composite was applied to modify the GCE, the R_{et} was decreased greatly (curve d), which proved that the assembly of the composite made the electron-transfer easier. These results could be attributed to the increased conductivity of the nitrogen-doped graphene (Yang et al., 2013b).

3.3. Electrocatalysis of glucose

The electrocatalytic activity of Nafion–Cu–N-G, Nafion–Cu and Nafion–N-G modified electrodes was recorded separately in 0.1 M NaOH solution with the absence and presence of 4 mM glucose at a scan rate of 50 mV s^{-1}. As shown in Fig. S6, no peak current was obtained in 0.1 M NaOH solution. Upon the addition of 4 mM glucose, it can be seen from Fig. 3A that an irreversible glucose oxidation peak at +0.68 V was obtained at the Nafion–Cu/GCE (curve b), and no obvious oxidation current can be found at Nafion–N-G/GCE (curve a). Moreover, Nafion–Cu–N-G/GCE exhibited enhanced electrocatalytic oxidation to glucose with the electrochemical response ca. 23-fold higher than that of pure Cu NPs (curve c). These results indicated that the Cu–N-G exhibited excellent electrocatalytic activity toward the oxidation of glucose as expected. Such excellent electrocatalytic activity of the Cu–N-G may be attributed to the introduction of N-G, which promote electron transfer in the oxidation of glucose.

Fig. 3B presented the CV responses obtained at Nafion–Cu–N-G/GCE in 0.1 M NaOH solution containing different concentrations of glucose at a scan rate of 50 mV s^{-1}. As can be seen in curve a, no oxidation peak was observed in the absence of glucose, upon the addition of 4 mM glucose (curve b), notable enhancement of oxidative peak current corresponding to the irreversible oxidation of glucose was observed, and the voltammetric response increased with a rising concentration of glucose at about +0.5 V (curve c), where the oxidation potential is due to the conversion of Cu(II) to Cu(III) (Wu et al., 2010; Yang et al., 2010). It has been proposed that Cu(III) species may act as an electron transfer mediator for the oxidation of glucose (Wu et al., 2010). Thus, the electrocatalytic mechanism of Cu–N-G towards glucose may be attributed to the involvement of Cu(II) and Cu(III) surface specie in the oxidation of glucose in alkaline medium. Moreover, the peak potential (+0.5 V) for glucose oxidation was more negative than that of Cu–graphene nanocomposite modified electrode (+0.65 V) in previous report (Chen et al., 2012).

3.4. Amperometric response of Nafion–Cu–N-G/GCE toward glucose

Fig. 4A illustrated amperometric response of Nafion–Cu–N-G/GCE for successive step changes of glucose concentration at +0.5 V. As the glucose was injected into 0.1 M NaOH, a step-style increase in current responses generated after each addition of glucose. It took less than 5 s (inset in Fig. 4B) to reach the steady-state current, indicating the fast amperometric response of the modified electrode. Moreover, Nafion–Cu–N-G/GCE displayed a wide linear response range from 4×10^{-6} M to 4.5×10^{-3} M with a correlation coefficient of 0.995, a high sensitivity of 48.13 μA mM^{-1}, and a detection limit of 1.3 μM at the signal-to-noise ratio of three. The above electrocatalytic studies of the biosensor revealed the properties of higher sensitivity and lower detection limit than Nafion–Cu/GCE in our previous study (Xu et al., 2011), which is due to the promoted electron transfer and superb catalytic activity afforded by N-G and Cu NPs.

3.5. Reproducibility, stability and anti-interference property of the biosensor

The reproducibility of the biosensor was examined by measuring the current responses upon 0.1 mM glucose in 0.1 M NaOH solution. In a series of five electrodes prepared in the same way, a relative standard deviation (RSD) of 5.8% was obtained, indicating the reliability of this method. While 5 measurements for a single electrode were made upon the addition of 0.1 mM glucose in 0.1 M NaOH with RSD of 3.9%, demonstrating excellent reproducibility.

In order to evaluate the stability of the biosensor, the current responses to 0.1 mM glucose were measured in 0.1 M NaOH solution at +0.5 V with every 2 days intervals. When it was not measured, the electrode could be washed with double distilled water and dried at room temperature in air. As shown in Fig. S7, the proposed biosensor retained about 88% of its initial response after three weeks, suggesting that the biosensor has good stability.

A number of oxidizable species such as AA, DA, AP, UA, and other carbohydrate compounds such as fructose, lactose and sucrose, usually co-exist with glucose in many samples, although at low concentrations relative to glucose, they exhibit high electron transfer rates and often interfere with the determination of glucose. Considering the concentration of glucose is at least 30

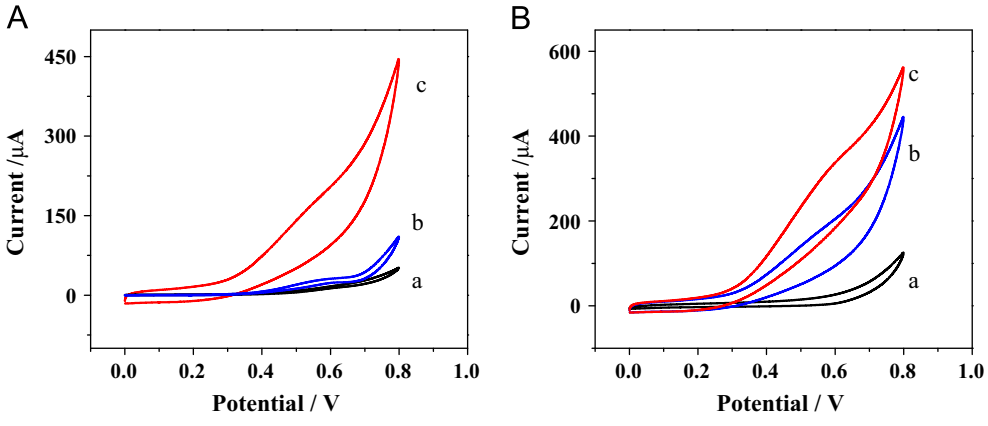

Fig. 3. (A) CVs of Nafion–N-G/GCE (a), Nafion–Cu/GCE (b) and Nafion–Cu–N-G/GCE (c) in 0.1 M NaOH solution containing 4 mM glucose at a scan rate of 50 mV s^{-1}. (B) CVs of Nafion–Cu–N-G/GCE in 0.1 M NaOH solution with 0 mM (a), 4.0 mM (b) and 8.0 mM (c) of glucose at the scan rate of 50 mV s^{-1}.

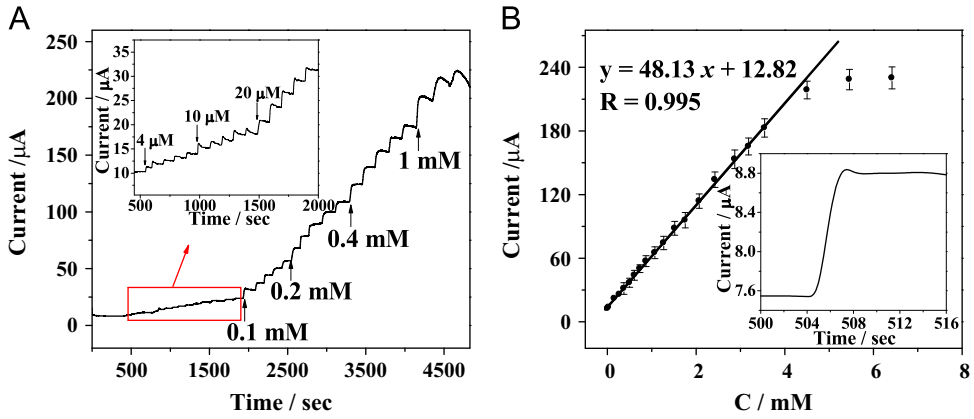

Fig. 4. (A) Amperometric response of Nafion–Cu–N-G/GCE for successive addition of various concentrations of glucose to 0.1 M NaOH at +0.5 V. Inset: amplification of the *i*–*t* curve. (B) The calibration curve for glucose detection. Inset: response time of the biosensor.

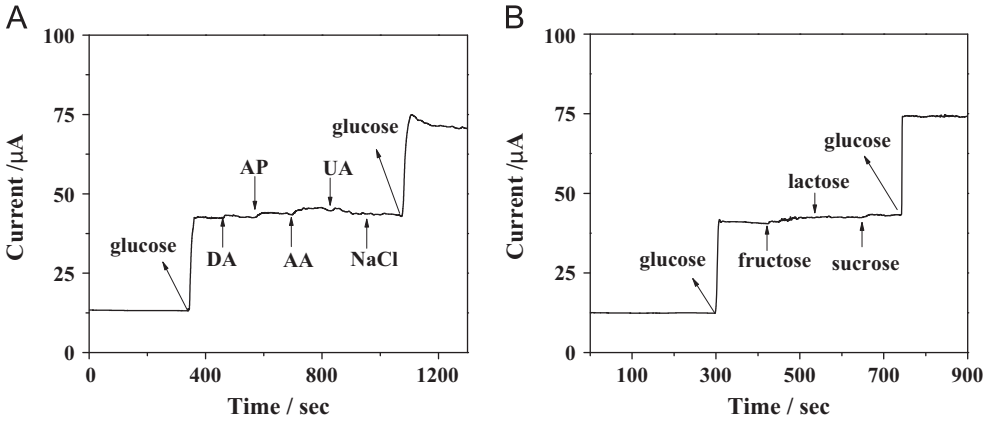

Fig. 5. (A) Interference test of Nafion–Cu–N-G/GCE in 0.1 M NaOH at +0.5 V with 1 mM glucose, 0.1 mM DA, 0.1 mM AP, 0.1 mM AA, 0.1 mM UA, 0.1 mM NaCl and 1 mM glucose. (B) Interference test of Nafion–Cu–N-G/GCE in 0.1 M NaOH at +0.5 V with 1 mM glucose, 0.1 mM fructose, 0.1 mM lactose, 0.1 mM sucrose and 1 mM glucose.

times of interfering species in human blood, the interference experiment was carried out by successive addition of 1.0 mM glucose and 0.1 mM interfering species in 0.1 M NaOH solution at a potential of +0.5 V. At the same time, the tolerance of Nafion–Cu–N-G/GCE to chloride was tested by adding 0.1 mM NaCl to the electrolyte. As can be seen from Fig. 5, the current responses for the interfering species to that of the glucose were below 4.8%, indicating that Nafion–Cu–N-G/GCE is highly specific to glucose even in the presence of several interfering species. Meanwhile, the addition of NaCl did not show any effect on the current of glucose oxidation, suggesting high chloride tolerance of Nafion–Cu–N-G/GCE.

3.6. Blood serum sample measurement

In order to explore the practicability of the biosensor, it was applied to determine the concentration of glucose in human blood serum samples of diabetic and healthy people, which were obtained from Jiang Bin hospital. 10 μL of blood serum sample was added to 5 mL 0.1 M NaOH solution with stirring and the final concentration was in the linear range of the proposed biosensor. Amperometric detection was carried out to measure the current response at the applied potential of +0.5 V by using the standard addition method and the results are shown in Table 1. The determined results of the blood serum samples are in accordance with those tested by hospital, indicating that the biosensor has a great potential for practical application for the analysis of glucose in real clinical samples.

Table 1
Results for determinations of glucose in blood serum samples (n=5).

Sample	Hospital (mM)	Our biosensor (mM)	RSD (%)	Added (mM)	Recovery (%)
1	5.1	5.17	2.9	0.5	103.4
2	12.3	12.45	4.7	0.5	101.9
3	4.7	4.63	3.4	0.5	99.8
4	6.0	5.97	2.6	0.5	97.6
5	4.9	5.02	4.1	0.5	102.3

Each sample was measured for three times.

4. Conclusions

In summary, the Cu–N-G was successfully prepared by a facile method via thermal treatment, and a novel non-enzymatic glucose sensor was fabricated based on the resulting Cu–N-G, which exhibited improved electrocatalytic activity to glucose oxidation than pure Cu NPs. The biosensor displayed excellent performances for glucose detection, such as wide linear range, low detection limit, high stability and perfect specificity to glucose in the presence of common interferents as well as avoiding poison by chloride ions. The relatively facile and low-cost fabrication of such

biosensor makes it as a potential candidate for routine glucose sensing.

Acknowledgments

The present work was supported by the National Natural Science Foundation of China (Nos. 21375050, 21175061, and 31271620), Major Program of Natural Science Foundation of Education Bureau of Jiangsu Province, China (Grant no. 10KJA470007), Key Laboratory of Modern Agriculture Equipment and Technology (No. NZ201109), China Post-doctoral Science Foundation (Nos. 2012M520998 and 2012M511217), Research Foundation of Jiangsu University (12JDG087) and Innovation Project of Science and Technology for College Graduates of Jiangsu Province (No. CXZZ12_0704).

Appendix A. Supporting information

Supplementary data associated with this article can be found in the online version at http://dx.doi.org/10.1016/j.bios.2013.11.005.

References

Borowiec, J., Wang, R., Zhu, L.H., Zhang, J.D., 2013. Electrochim. Acta 99, 138–144.
Cherevko, S., Chung, C.H., 2012. Sens. Actuators B 142, 216–223.
Chen, Q.W., Zhang, L.Y., Chen, G., 2012. Anal. Chem. 84, 171–178.
Chen, X.M., Cai, Z.M., Lin, Z.J., Jia, T.T., Liu, H.Z., Jiang, Y.Q., Chen, X., 2009. Biosens. Bioelectron. 24, 3475–3480.
Delvaux, M., Champagne, S.D., 2003. Biosens. Bioelectron. 18, 943–951.
Gilje, S., Han, S., Wang, M.S., Wang, K.L., Kaner, R.B., 2007. Nano Lett. 7, 3394–3397.
Guo, H.L., Su, P., Kang, X.F., Ning, S.K., 2013. J. Mater. Chem. A 1, 2248–2255.
Higgins, D., Chen, Z., Lee, D.U., Chen, Z.W., 2013. J. Mater. Chem. A 1, 2639–2645.
Hu, Y.W., Wang, K.K., Zhang, Q.X., Li, F.H., Wu, T.S., Niu, L., 2012. Biomaterials 33, 1097–1106.
Jin, J.T., Fu, X.G., Liu, Q., 2013. ACS Nano 6, 4764–4773.
Kang, X.H., Mai, Z.B., Zou, X.Y., Cai, P.X., Mo, J.Y., 2007. Anal. Biochem. 363, 143–150.
Kung, C.W., Lin, C.Y., Lai, Y.H., Vittal, R., Ho, K.C., 2011. Biosens. Bioelectron. 27, 125–131.
Luo, J., Jiang, S.S., Zhang, H.Y., Jiang, J.Q., Liu, X.Y., 2012. Anal. Chim. Acta 709, 47–53.
Qiu, J.D., Wang, R., Liang, R.P., Xia, X.H., 2009. Biosens. Bioelectron. 24, 2920–2925.
Sreedhar, B., Radhika, P., Neelima, B., Hebalkar, N., 2008. Chem. Asian. J. 3, 1163–1169.
Steiner, M., Duerkop, A., Wolfbeis, O.S., 2011. Chem. Soc. Rev. 40, 4805–4839.
Sun, F., Li, L., Liu, P., 2011. Electroanalysis 23, 395–401.
Valentini, F., Fernandez, L.G., Tamburri, E., Palleschi, G., 2013. Biosens. Bioelectron. 43, 75–78.
Vinayan, B.P., Nagar, R., Rajalakshmi, N., Ramaprabhu, S., 2012. Adv. Funct. Mater. 22, 3519–3526.
Wang, G.F., He, X.P., Wang, L.L., Gu, A.X., Huang, Y., Fang, B., Geng, B.Y., Zhang, X.J., 2013. Microchim. Acta 180, 161–186.
Wang, X., Hu, C.G., Liu, H., Gu, G.J., He, X.S., Xi, Y., 2010. Sens. Actuators B 144, 220–225.
Wu, H.X., Cao, W.M., Li, Y., 2010. Electrochim. Acta 55, 3734–3740.
Wu, Q., Wang, L., Yu, H., Wang, J., Chen, Z., 2011. Chem. Rev. 111, 7855–7875.
Wu, G.H., Song, X.H., Wu, Y.F., Chen, X.M., Luo, F., Chen, X., 2013. Talanta 105, 379–385.
Xiong, B., Zhou, Y.K., Zhao, Y.Y., Wang, J., Chen, X., O'Hayre, R., Shao, Z.P., 2013. Carbon 52, 181–192.
Xu, L., Xia, J.X., Li, H.M., Li, H.N., Wang, K., Yin, S., 2011. Eur. J. Inorg. Chem. 2011, 1361–1365.
Yang, G.H., Li, L.L., Rana, R.K., Zhu, J.J., 2013a. Carbon 61, 357–366.
Yang, J., Zhang, W.D., Gunasekarana, S., 2010. Biosens. Bioelectron. 26, 279–284.
Yang, S.H., Song, X.F., Zhang, P., Gao, L., 2013b. ACS Appl. Mater. Interface 5, 3317–3322.
Yang, Z.Y., Feng, J.S., Qiao, J.S., Yan, Y.Y., 2012. Anal. Methods 4, 1924–1926.
Zhang, Y.C., Su, L., Manuzzi, D., Jia, W.Z., Huo, D.Q., Hou, C.J., Lei, Y., 2012. Biosens. Bioelectron. 31, 426–432.
Zhao, J., Wei, L.M., Peng, C.H., 2013. Biosens. Bioelectron. 47, 86–91.
Zhou, X.M., Nie, H.G., Yao, Z., Dong, Y.Q., Yang, Z., Huang, S.M., 2012. Sens. Actuators B 168, 1–7.